Sciencexpress Report

The Hot Summer of 2010: Redrawing the Temperature Record Map of Europe

David Barriopedro,[1]* Erich M. Fischer,[2] Jürg Luterbacher,[3] Ricardo M. Trigo,[1] Ricardo García-Herrera[4]

[1]Instituto Dom Luiz, University of Lisbon, Portugal. [2]Institute for Atmospheric and Climate Science, ETH Zurich, Switzerland. [3]Department of Geography, Justus-Liebig-University of Giessen, Germany. [4]Agencia Estatal de Meteorología (AEMET), Madrid, Spain.

*To whom correspondence should be addressed. E-mail: dbarriopedro@fc.ul.pt

The summer of 2010 was exceptionally warm in eastern Europe and large parts of Russia. We provide evidence that the anomalous 2010 warmth that caused adverse impacts exceeded the amplitude and spatial extent of the previous hottest summer of 2003. 'Mega-heatwaves' such as the 2003 and 2010 events broke the 500-yr long seasonal temperature records over approximately 50% of Europe. According to regional multi-model experiments, the probability of a summer experiencing 'mega-heatwaves' will increase by a factor of 5 to 10 within the next 40 years. However, the magnitude of the 2010 event was so extreme that despite this increase, the occurrence of an analogue over the same region remains fairly unlikely until the second half of the 21st century.

Increasing greenhouse gas concentrations are expected to amplify the variability of summer temperatures in Europe (*1–5*). Along with mean warming, enhanced variability results in more frequent, persistent and intense heatwaves (*6–10*). Consistent with these expectations, Europe has experienced devastating heatwaves in recent years. The exceptional summer of 2003 (*1*, *11–13*) caused around 70,000 heat-related deaths mainly in western and central Europe (*14*). In summer 2010 many cities in eastern Europe recorded extremely high values of daytime (e.g. Moscow: 38.2ºC), nighttime (e.g. Kiev: 25ºC) and daily mean (e.g. Helsinki: 26.1ºC) temperatures (fig. S1). Preliminary estimates for Russia referred a death toll of 55,000, an annual crop failure of ~25%, more than 1 million ha of burned areas and ~US$15 billion (~1% GDP) of total economic loss (*15*). During the same period, parts of eastern Asia also experienced extremely warm temperatures and Pakistan was hit by devastating monsoon floods.

In order to characterize the magnitude and spatio-temporal evolution of the 2010 event in a historical context, we used daily mean datasets from the two longest reanalyses, which together back to 1871 (*15–17*). The spatial pattern of the maximum summer temperature anomalies (Fig. 1, A to D) reveals that western Russia was in the center of the exceptional warmth at all temporal scales. Weekly to monthly anomalies were particularly pronounced, exceeding the 1970-1999 mean (*18*) by 10ºC, i.e. more than 4 standard deviations (SDs). According to reanalyses, other countries (Baltic countries, Belarus, Ukraine and Kazakhstan) also experienced extreme temperatures that broke the summer records of the last 140 years at many temporal scales (see also SOM text).

Figure 1e displays the temporal evolution of areas that were simultaneously affected by record-breaking anomalies for any summer period of 1-day to 91-day length. At short time-scales (daily to fortnightly), new historical maxima were first observed in late July 2010 and persisted until the second week of August. During that time, extensive fires across western Russia killed 53 people and made 3,500 people homeless, and Moscow suffered a devastating rise in mortality, smoke fire and air pollution (*15*). The record-breaking pattern is not symmetric in time, indicating that warm conditions had started already in July and ended abruptly by mid-August. Between mid-July and early August, a record-scale area of more than 2,000,000 km^2 registered unprecedented anomalies at the 15-day to 61-day time-scales. These results reflect the extraordinary nature of the 2010 event and confirm that most of the record-breaking values highlighted in Figure 1a-d occurred simultaneously.

The most evident features associated with the 2010 event were: (i) quasi-stationary anticyclonic circulation anomalies over western Russia (fig. S5); (ii) deficit of January-to-July 2010 accumulated precipitation and early spring snow cover disappearance in western-central Russia (fig. S6). High-pressure systems are well-known to produce warm conditions at surface by enhancing subsidence, solar heating and warm-air advection (*19–21*). The lack of water availability results in a continuous reduction of soil moisture and enhanced sensible heat fluxes that exacerbate the strength of summer heatwaves (*20–22*).

Unlike 2010, the summer of 2003 was characterized by two extreme periods (centered on 15 June and the first fortnight of August) (*12*) that contributed to rise the number of locations with temperatures beyond their historical maxima at seasonal time-scales. However, the 2010 event exceeded the 2003 episode in terms of amplitude and spatial extent.

Thus, the maximum extension of areas experiencing record-breaking temperatures in 2003 was ~1,000,000 km^2, considerably lower than that of 2010. The intensity of the 2003 event was also ~1-2 SDs weaker for almost any subseasonal time-scale (fig. S7).

Despite the distinctive spatio-temporal evolution of the 2003 and 2010 events, their record-breaking anomalies reached comparable amplitude and extension at seasonal scales. Therefore, from a seasonal perspective, it is interesting to compare how these events impacted at continental scales. Herein, surface temperature analysis data (*23*) and multiproxy surface air temperature reconstructions since 1500 (*11*) are used to place these recent extreme European summers in a palaeoclimatic context (*15*). Figure 2 displays the European mean summer land surface air temperature distribution for the 1500-2010 period. The European mean 2010 summer (ΔT=+1.8ºC, 3.5 SDs relative to 1970-1999) was ~0.2°C warmer than the previous warmest summer of 2003 (*11*). This number is even more noticeable if we consider that the European average temperature is defined for the land area [35ºN, 70ºN] and [25°W, 40°E], thus excluding many regions affected by outstanding temperatures in 2010. Further, the historical evolution of the hottest summers in Europe (Fig. 2, bottom panel) suggests that the last decade stands significantly above any other 10-yr period since 1500. Taking into account the uncertainties in the reconstruction (*11*, *15*), we find that at least two summers in this decade have most likely been the warmest of the last 510 years in Europe.

Figure 3 further stresses the exceptional magnitude of the 2010 summer, displaying the amplitude of the hottest summers across Europe and the decade when they occurred. To highlight the contribution of summers in the 2001-2010 decade, the analysis was initially restricted to the 1500-2000 period (Fig. 3A) and then updated to 2010 (Fig. 3B). Until the end of the 20th century (20C), maximum seasonal temperatures across Europe mostly ranged 2-3 SDs of their 1970-1999 climatology, with record-holder summers clustering in a few decades of the last five centuries. During the 2001-2010 decade, 500-yr long records were broken over ~65% of Europe, including eastern Europe (2010), southwestern-central Europe (2003), the Balkans (2007) and Turkey (2001). These summers have considerably contributed to the upper tail of the European distribution of summer maxima (Fig. 3, inset plot). Thus, the percentage of European regions with seasonal maxima above 3 SDs (>99th percentile of the 1970-1999 distribution) has doubled within one decade. The 2003 and 2010 summers were the warmest on record over ~25% of Europe, standing as the major contributors to the current European map of the hottest summers.

It is noticeable that the two hottest summers in Europe resulted from subseasonal heatwaves of outstanding magnitude and large spatial extent. This raises the question whether these 'mega-heatwaves' (*24*) (and regional extreme events at other time-scales) will become more frequent in the future. To address this question, we evaluate transient experiments from 11 high-resolution Regional Climate Models (RCMs) driven with different General Circulation Models (GCMs), which are forced with the A1B emission scenario (*15*, *25*). The analysis emphasizes analogues of the 2010 and 2003 events over the eastern (EE) and western (WE) European regions that were strongly impacted by these 'mega-heatwaves' (fig. S11).

Anthropogenic changes are assessed in terms of return periods (RPs) (*26*) of maximum 7-day summer regional temperature for three time slices (1970-1999, 2020-2049 and 2070-2099) (Fig. 4). Regional mean temperature were normalized with reference to the 1970-1999 climatology and hereafter expressed as SDs (*27*). Simulations for the 1970-1999 period indicate a reasonable model skill, although there is a considerably spread of model results, particularly for long RPs (figs. S12, S13). The ensemble of RCMs projects that weekly heat spells of the magnitude of the second week of August 2003 (7-day anomaly of 3.7 SDs), which are extremely rare in the 20C simulations, will likely occur in 2020-2049, with a best guess RP of ~10-yr in EE and ~15-yr in WE. However, a weekly 2010-like event (~4.5 SDs) remains unlikely in the same period (best guess RPs>30-yr over both regions). By the end of the 21st century (21C), such extreme weekly heat spells are expected every ~8 years in EE and ~4 years in WE, while some models show regular 2003-like anomalies (about every second summer). It should be noted that the estimated RPs involve major model uncertainties and should be carefully interpreted given the high natural variability of such extreme events. Thus, some RCMs show several events similar to 2010 in the period 2020-2049 (fig. S14, left) while others just one event similar to 2003 within the last 30 years of the 21C (fig. S14, right).

The increase in probability of 2003- and 2010-type events depends on the time-scale addressed and differs if the seasonal anomaly is emphasized instead of the weekly time-scale above (SOM text). The analysis of RCM time series for the 2011-2100 period reveals 2003 analogues (even at monthly and seasonal scales) before 2050 in more than half of the models (figs. S14 and S15). However, the same cannot be stated for a 2010 analogue until the second half of the 21C, particularly at monthly and seasonal scales. For the last 30 years of the 21C, the occurrence of 2010-like monthly anomalies (~5 SDs) increases rapidly to one event per decade in most models, and by 2100 all models present at least one summer like 2010.

The enhanced frequency for small to moderate anomalies of 2-3 SDs is mostly accounted for by a shift in mean summer temperatures (compare Fig. 4 with fig. S18). However, the

future probabilities of 'mega-heatwaves' with SDs similar to 2003 and 2010 are substantially amplified by enhanced variability. Particularly in WE, variability has been suggested to increase at interannual and intraseasonal time-scales (*1*, *2*) as a result of increased land-atmosphere coupling (*28*) and changes in the surface energy and water budget (*2*, *29*). Models indicate that the structure of circulation anomalies associated with 'mega-heatwaves' remains essentially unchanged in the future (SOM text).

Our results reveal that, along with the reported changes in local heatwaves (*8*), there is an increasing likelihood of 'mega-heatwaves' over highly populated areas of Europe with magnitudes such that they would exceed the exceptional current seasonal maxima of western Europe within the next four decades and of eastern Europe afterwards. Given the disastrous effects of the 2003 and 2010 events, these results venture serious risks of simultaneous adverse impacts over large areas if no adaptive strategies are adopted.

References and Notes

1. C. Schär *et al*., *Nature* **427**, 332 (2004).
2. E. M. Fischer, C. Schär, *Clim. Dyn*. **33**, 917 (2009).
3. J. H. Christensen *et al.*, Regional Climate Projections, in *Climate Change 2007: The Physical Science Basis. Contribution of Working Group I to the Fourth Assessment Report of the Intergovernmental Panel on Climate Change*, S. Solomon *et al.*, Eds. (Cambridge Univ. Press, New York, 2007).
4. F. Giorgi, X. Q. Bi, J. Pal, *Clim. Dyn*. **23**, 839 (2004).
5. A. Klein-Tank, G. Können, F. Selten, *Int. J. Climatol*. **25**, 1 (2005).
6. P. M. Della-Marta, M. R. Haylock, J. Luterbacher, H. Wanner, *J. Geophys. Res*. **112**, D15103 (2007).
7. G. A. Meehl, C. Tebaldi, *Science* **305**, 994 (2004).
8. E. M. Fischer, C. Schär, *Nature Geosci.* **3**, 398 (2010).
9. M. Beniston *et al., Clim. Change* **81**, 71 (2007).
10. F. G. Kuglitsch *et al., Geophys. Res. Lett.* **37**, L04802 (2010)
11. J. Luterbacher, D. Dietrich, E. Xoplaki, M. Grosjean, H. Wanner, *Science* **303**, 1499 (2004).
12. R. García-Herrera, J. Díaz, R. M. Trigo, J. Luterbacher, E. M. Fischer, *Crit. Rev. Environ. Sci. Technol*. **40**, 267 (2010).
13. E. Black, M. Blackburn, G. Harrison, B. Hoskins, J. Methven, *Weather* **59**, 217 (2004).
14. J. M. Robine *et al*., *C. R. Biol*. **331**, 171 (2008).
15. Materials and methods are available as supporting material on *Science* Online.
16. R. Kistler *et al*., *Bull. Am. Meteorol. Soc.* **82**, 247 (2001).
17. G. P. Compo *et al*., *Q. J. R. Meteorol. Soc.* **137**, 1–28 (2011).
18. For coherence with model results, and due to the limited availability of data in some models, 1970-1999 is used as the reference period throughout this manuscript. Summer includes all days from 1 June to 31 August.
19. R. M. Trigo, R. García-Herrera, J. Díaz, I. F. Trigo, M. A. Valente, *Geophys. Res. Lett*. **32**, L10701, doi:10.1029/2005GL022410 (2005).
20. E. Xoplaki, J. F. González-Rouco, J. Luterbacher, H. Wanner, *Clim. Dyn*. **20**, 723 (2003).
21. E. M. Fischer, S. I. Seneviratne, D. Lüthi, C. Schär, *Geophys. Res. Lett*. **34**, L06707, doi:10.1029/2006GL029068 (2007).
22. R. Vautard *et al*., *Geophys. Res. Lett*. **34**, L07711, doi:10.1029/2006GL028001 (2007).
23. J. Hansen, R. Ruedy, J. Glascoe, M. Sato, *J. Geophys. Res.* **104**, 30997 (1999).
24. The concept of 'mega-heatwave' is herein used to refer to regional mean temperature anomalies (over ~1 million km^2) of extraordinary amplitude (approximately ≥3 SDs) at subseasonal scales (of at least 7-day), thus differing from the classic local heatwave definition.
25. P. van der Linden, J.F.B. Mitchell, "ENSEMBLES: Climate Change and its Impacts: Summary of research and results from the ENSEMBLES project" (Met. Office Hadley Centre, Fitzroy Road, Exeter EX1 3PB, UK, 2009).
26. S. G. Coles, *An Introduction to Statistical Modeling of Extreme Values* (Springer, London, 2001).
27. Note that summer temperature variability is higher in EE, and hence, a given value in SDs actually implies larger anomalies in EE than in WE.
28. S.I. Seneviratne, D. Lüthi, M. Litschi, C. Schär, *Nature* **443**, 205 (2006).
29. G. Lenderink, A. van Ulden, B. van den Hurk, E. van Meijgaard, *Clim. Change* **81**, 233 (2007).

30. Acknowledgements. This study was supported by the EU/FP6 project CIRCE (#036961) (DB, JL, RT, RG), the IDL-FCUL project ENAC (PTDC/AAC-CLI/103567/2008) (DB, RT), the Swiss National Science Foundation (NCCR Climate) (EF), the EU/FP7 project ACQWA (#212250) (JL), the DFG project PRIME within the Priority Program 'INTERDYNAMIK' (JL) and the project 'Klimawandel und Extremwetter in Hessen – Analyse von Beobachtungsdaten des 20. Jahrhunderts und Ensembleprojektionen für das 21. Jahrhundert' funded by the Hessian Centre on Climate Change and Geology (JL). The ENSEMBLES data used in this work was funded by the EU/FP6 project ENSEMBLES (#505539) whose support is gratefully acknowledged.

Supporting Online Material

www.sciencemag.org/cgi/content/full/science.1201224
Materials and Methods
SOM text

Figs. S1 to S18
Table S1
References and Notes

3 December 2010; accepted 2 March 2011
Published online 17 March 2011; 10.1126/science.1201224

Fig. 1. Spatio-temporal evolution of the 2010 summer. Maximum temperature anomalies (ºC, relative to 1970-1999) in summer 2010 for: a) 7-day; b) 15-day; c) 31-day; d) 61-day average periods. Contour lines indicate the anomaly divided by the corresponding standard deviation of all summer days of the reference period. Black points highlight record-breaking values, the size being proportional to exceedance over the previous maximum. The maximum record-breaking temperature anomaly is shown in the upper left corner; e) Temporal evolution of the spatial extent (in 10^3 km^2) of areas experiencing record-breaking temperatures at different time-scales during summer 2010. Only those regions within the box of Fig.1d are considered. Blue bars indicate the period of maximum extension for the time-scales represented in Fig.1a-d. Data are from (*17*) (1871-1947) and (*16*) (1948-2010).

Fig. 2. European summer temperatures for 1500-2010. Statistical frequency distribution of European ([35ºN, 70ºN], [25ºW, 40ºE]) summer land temperature anomalies (ºC, relative to the 1970-1999 period) for the 1500-2010 period (vertical lines). The five warmest and coldest summers are highlighted. Grey bars represent the distribution for the 1500-2002 period (*11*) with a Gaussian fit in black. Data for the 2003-2010 period are from (*23*). The bottom panel shows the running decadal frequency of extreme summers, defined as those with temperature above the 95th percentile of the 1500-2002 distribution. A 10-yr smoothing is applied. Dotted line shows the 95th percentile of the distribution of maximum decadal values that would be expected by random chance (*15*).

Fig. 3. Spatial distribution of the hottest European summers. The height and the color of the bars indicate the anomaly (ºC, relative to the 1970-1999 period) and the decade of the corresponding summer, respectively, for the period: a) 1500-2000; b) 1500-2010. For better readability, each bar is subdivided with 1ºC intervals. The embedded plot shows the percentage of European areas with summer maxima above the given temperature (in SDs) for the 1500-2000 (dashed line) and 1500-2010 (dotted line) periods. Data sources are (*11*) (1500-2002) and (*23*) (2003-2010).

Fig. 4. Multi-model projections of 'mega-heatwaves'. Return periods (years) of 7-day summer maximum regional temperature for three 30-yr periods and 11 RCMs (*25*) over: a-c) EE ([52.5ºN, 60ºN]; [27.5ºE, 40ºE]); d-f) WE ([42.5ºN, 50ºN]; [0ºE, 15ºE]). Anomalies are depicted as standard deviations of the control period 1970-1999. Shading indicates the degree of agreement between models as measured by the overlapping of their 95% confidence interval limits. Dotted lines comprise the 75% density distribution, with the median in between. Black lines represent the corresponding fit from reanalysis (*16*). Blue and green dots represent the RCM-projected distribution of RPs for a 2010- and a 2003-like event, respectively, with the size proportional to the level of model agreement. The vertical mark indicates the best guess, as obtained from the median of the RCM distribution.

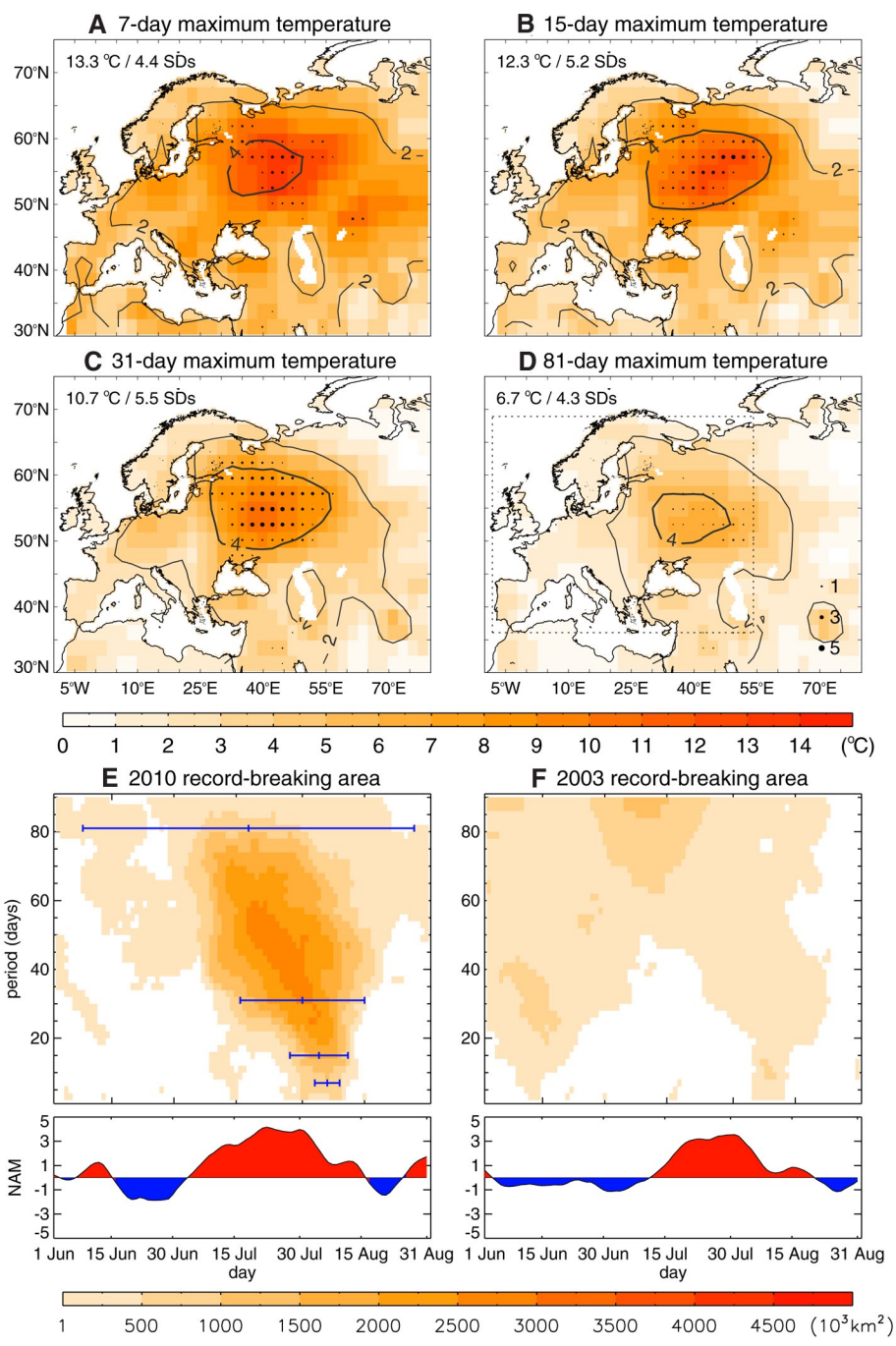
A 7-day maximum temperature
13.3 ℃ / 4.4 SDs
B 15-day maximum temperature
12.3 ℃ / 5.2 SDs
C 31-day maximum temperature
10.7 ℃ / 5.5 SDs
D 81-day maximum temperature
6.7 ℃ / 4.3 SDs
70°N
60°N
50°N
40°N
30°N
5°W
10°E
25°E
40°E
55°E
70°E
0 1 2 3 4 5 6 7 8 9 10 11 12 13 14 (℃)
E 2010 record-breaking area
F 2003 record-breaking area
period (days)
NAM
1 Jun 15 Jun 30 Jun 15 Jul 30 Jul 15 Aug 31 Aug
day
1 500 1000 1500 2000 2500 3000 3500 4000 4500 (10^3km^2)

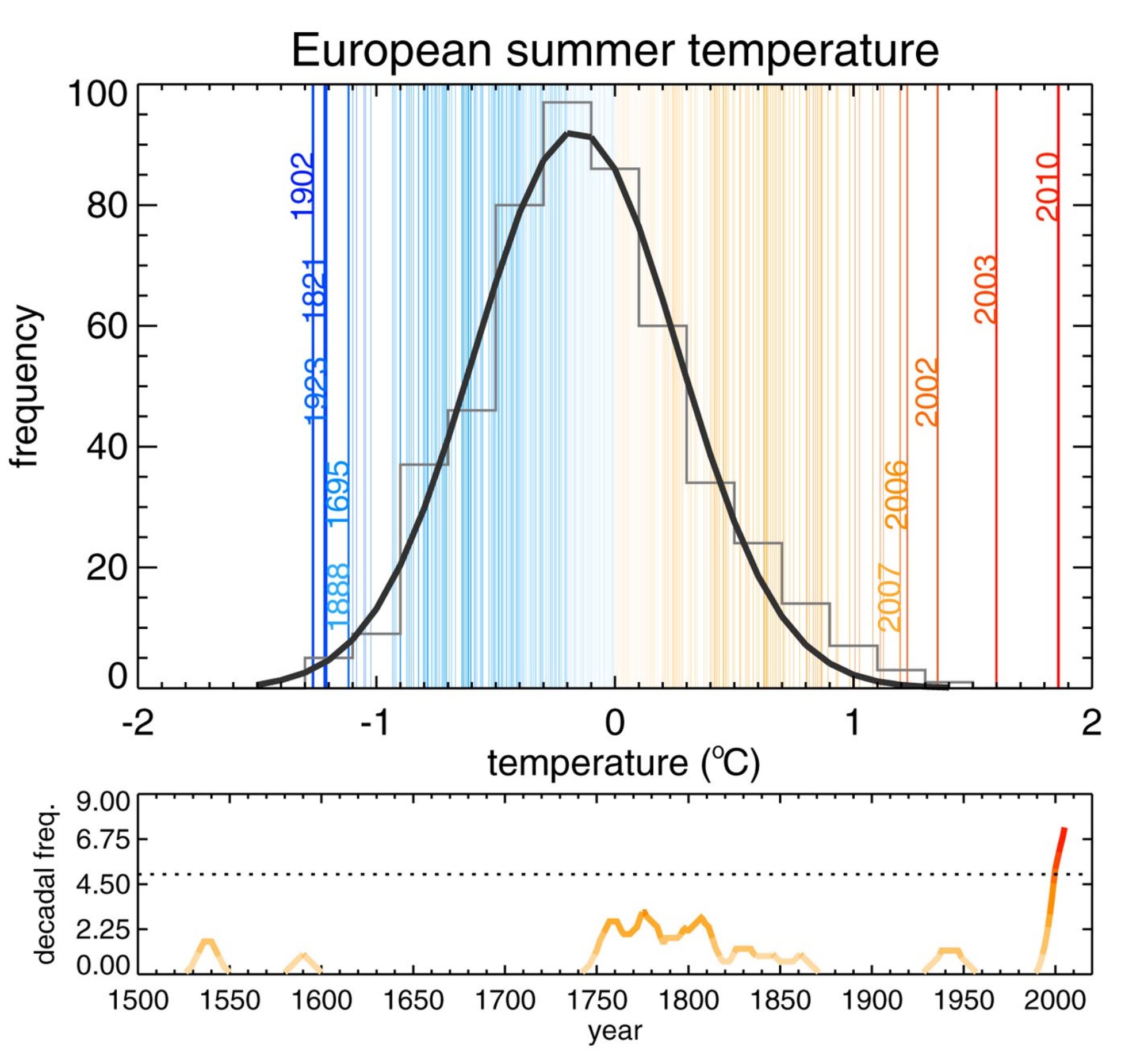
European summer temperature
frequency
100
80
60
40
20
0
1902
1821
1923
1695
1888
2010
2003
2002
2006
2007
-2
-1
0
1
2
temperature (°C)
decadal freq.
9.00
6.75
4.50
2.25
0.00
1500
1550
1600
1650
1700
1750
1800
1850
1900
1950
2000
year

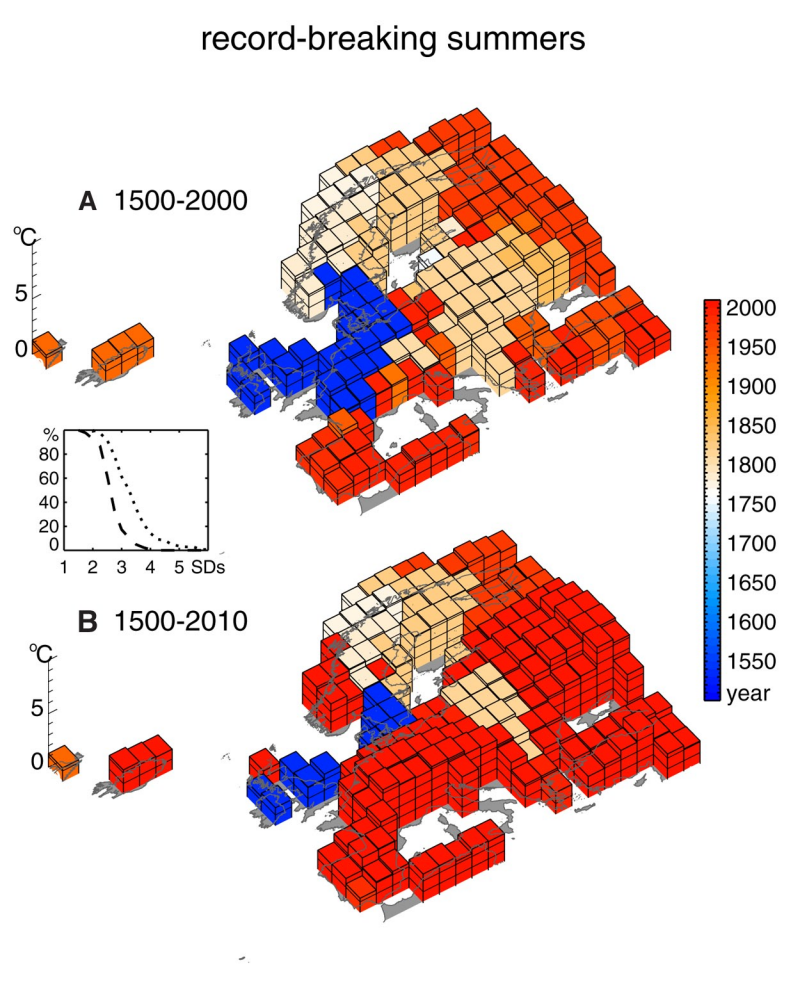
record-breaking summers
A 1500-2000
°C
5
0
%
80
60
40
20
0
1 2 3 4 5 SDs
2000
1950
1900
1850
1800
1750
1700
1650
1600
1550
year
B 1500-2010
°C
5
0

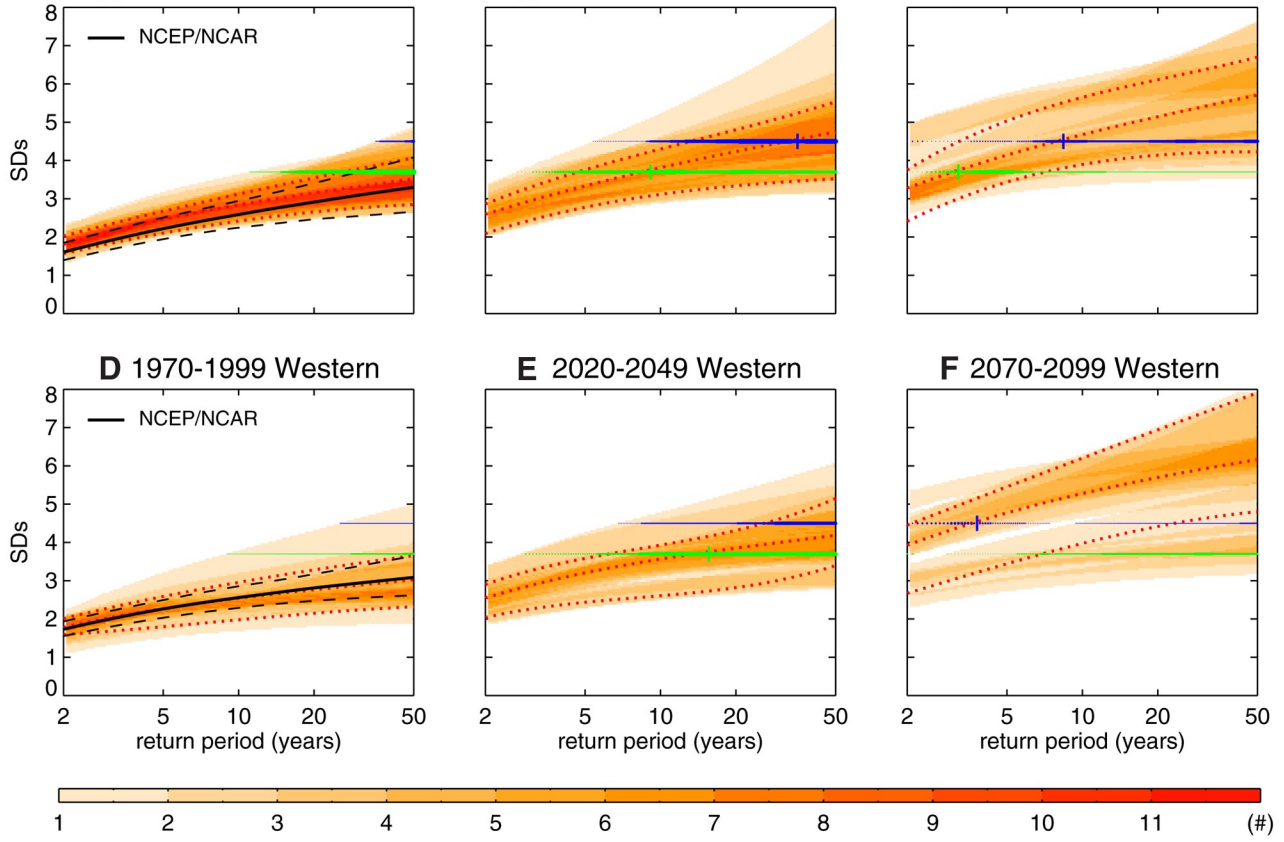
A 1970-1999 Eastern
B 2020-2049 Eastern
C 2070-2099 Eastern
D 1970-1999 Western
E 2020-2049 Western
F 2070-2099 Western
NCEP/NCAR
SDs
return period (years)
2
5
10
20
50
0
1
2
3
4
5
6
7
8
(#)